Ocean Sci. Discuss., 12, 449–492, 2015
www.ocean-sci-discuss.net/12/449/2015/
doi:10.5194/osd-12-449-2015

Ocean Science
Discussions
Open Access

The Barents Sea polar front and water masses variability (1980–2011)

L. Oziel, J. Sirven, and J.-C. Gascard

Sorbonne Universités (UPMC, Univ. Paris 06)-CNRS-IRD-MNHN, LOCEAN Laboratory, IPSL, Université Pierre et Marie Curie, 75005, Paris, France

Received: 12 February 2015 – Accepted: 20 February 2015 – Published: 10 March 2015

Correspondence to: L. Oziel (laurent.oziel@locean-ipsl.upmc.fr)

Published by Copernicus Publications on behalf of the European Geosciences Union.

Abstract

The polar front separates the warm and saline Atlantic Waters encountered in the western part of the Barents Sea from the cold and fresh Arctic Waters situated in the northern part. These water masses can mix together, mainly in the eastern part of the Barents Sea, generating dense waters in winter which can cascade into the Arctic Ocean to form the Artic Intermediate Waters. To study the interannual variability and evolution of these water masses and the fronts, we have merged data from the International Council for the Exploration of the Sea and the Arctic and Antarctic Research Institute and have built a new database which covers the period 1980–2011. The summer data is interpolated on a regular grid and a "Probability Density Function" method is used to show that the polar front splits into two branches east of 32° E where the topographic constraint weakens. Two fronts can then be defined: the "Northern Polar Front" is associated with strong salinity gradients and the "Southern Polar Front" with temperature gradients. They enclose the dense Barents Sea Water. The interannual variability of the water masses is apparent in the observed data and is linked to that of the ice cover. In contrast, the link with the Arctic Oscillation is not clear. However, results from a general circulation model suggest that such a link could be found if winter data were taken into account. A strong trend, which amplifies during the last decade, is also found: the Atlantic Water occupies a larger volume of the Barents Sea. This "Atlantification" could be accompanied by a northwards displacement of the southern polar front in the eastern part of the Barents Sea (which is suggested by a model based study) and a decrease of the volume occupied by the Arctic Waters.

OSD

12, 449–492, 2015

1 Introduction

1.1 The Barents Sea: a key region for the water mass transformations

The Barents Sea (BS) extends over the northernmost Arctic shelf; it has a mean depth of about 230 m and covers about 1.4 million km^2 (Fig. 1a). The water mass distribution is strongly constrained by the cyclonic circulation, which dominates the BS (Fig. 1b), and the bottom topography, especially in the shallow areas. This circulation is forced by the Atlantic Waters (AW) and the Norwegian Coastal Current Waters which inflow to the BS through the Barents Sea Opening (BSO); a shelf break which is 470 m deep at the deepest point. These Eastward inflows amount to about 2 Sv (Ingvaldsen et al., 2002) and 1.1 Sv (Skagseth, 2008) respectively. Tides of high intensity are observed in the BS, principally in shallow and coastal areas (like the Svalbard or the Norwegian coast). They induce a significant turbulent mixing.

The warm and saline Atlantic Waters mixes in the BS with the fresh and cold Arctic Waters (ArW) and with the Norwegian Coastal Current Waters along the Norwegian coast (see Gascard et al., 2004, and Fig. 1b). This sea thus plays a key role in the mass water transform and is subject to large hydrological contrasts. The salinity is affected by the saline Atlantic Waters which inflows from the Norwegian Sea and the fresh water issuing from the Norwegian Coastal Current Waters, Arctic Waters, rivers, and ice melting, and can range from 33 to 35.2. The temperature also varies significantly, ranging from −1.8 °C for the Arctic Waters (freezing point) to more than 10 °C for the Norwegian Coastal Current Waters at surface during summer.

The cooling and mixing of the Atlantic Waters, Arctic Waters and Norwegian Coastal Current Waters, reinforced by brines rejections due to ice formation (especially around Svalbard, Franz Josef Land and Novaya Zemlya) and favorable conditions for shelf convection (Martin and Cavalieri, 1989), produce the dense Barents Sea Waters (BSW). They mostly flow into the Arctic Ocean on the sea bottom between Novaya Zemlya (60° E, 76° N) and Franz Josef Land (60° E, 80° N) and partly contribute to the overturning circulation of the North Atlantic (Anderson et al., 1999). The Barents Sea Wa-

OSD
12, 449–492, 2015

ters also provide intermediate waters to the Arctic Ocean at a depth of about 1200 m (Rudels et al., 1994; Schauer et al., 1997, 2002). All of these features and processes can be affected by the climate change. Note that dense waters are also produced in the Storfjord (Svalbard), but they flow into the Arctic Ocean through the Fram strait, to the west of the Svalbard. We do not consider them in this paper.

1.2 Climate change and low frequency variability of the Barents Sea

During the past decade (1998–2008), the BS has experienced the largest reduction of sea ice cover in the Arctic (Screen and Simmonds, 2010) coupled with an air-ice–ocean system warming (Serreze et al., 2007). The annual sea ice extent has decreased by 50 %, reaching its lowest level for the last 60 years (Årthun et al., 2012). The BS is becoming the first "ice-free" Arctic Sea (with the Baffin Bay) in summer and autumn. In winter and spring, a seasonal Marginal Ice Zone remains in the northern and sometimes eastern part of the BS, close to Novaya Zemlya. The north-eastern BS is the region where the sea ice variability is the largest (Inoue et al., 2012).

As the sea ice extent decreases, the air–sea exchanges in the BS increase. The low frequency variability of the Arctic is commonly associated with the Arctic Oscillation (AO) (Thompson and Wallace, 1998). A negative (positive) AO generally corresponds to a cold (warm) atmospheric event over the eastern Arctic, a high (low) pressure anomaly and an anticyclonic (cyclonic) mode of the atmospheric circulation. The AO (Proshutinsky and Johnson, 1997) affects in particular the conditions along the western edge of the BS by modifying the Atlantic Waters inflow through the BSO, between Fugloya and Bjornoya, and consequently the circulation in the BS. Indeed, a higher pressure over the Arctic (corresponding to a negative AO) strengthens the westerly winds in the inflow area and then increases the Atlantic Waters penetration in the BS (Ingvaldsen et al., 2004). This would bring warmer Atlantic Waters, decrease sea ice extent, enhance heat loss from the ocean to the atmosphere, and increase fresh water content coming from the ice melting.

OSD
12, 449–492, 2015

Impacts of the interannual variability of the AO on the water mass transformations in the BS are still in debate. If the BS becomes warmer (and saltier), the stratification becomes stable since more ice is melting; hence, the mixing, which facilitates the formation of the Barents Sea Waters, is inhibited. In contrast, cold conditions favor winter ice production which releases a large amount of salt, making the water denser. The production of Barents Sea Waters would then be intensified.

1.3 Objectives

The BS plays an important role in the Northern Hemisphere climate (Smedsrud et al., 2013) by ventilating the Arctic Ocean with the dense Barents Sea Waters (Aagaard and Woodgate, 2001; Schauer et al., 2002) and by being a place of high primary productivity (Loeng, 1991). The BS water masses delimited by several fronts are of particular interest. In this paper, we try to specify the mean state and variability for the last 30 years (1980–2011) of:

1. The water masses distribution in a context of "Atlantification". This process, pointed out by Årthun et al. (2012) for the last decade, is defined by this author as an increase of the heat transport from the Atlantic towards the BS due to an increase of the Atlantic Waters transport and temperature.

2. The fronts associated with the Atlantic Waters, Arctic Waters, and Barents Sea Waters. These fronts constitute a major oceanographic feature of the BS (Johannessen and Foster, 1978; Pfirman et al., 1994; Gawarkiewicz and Plueddemann, 1995) and are associated with some vertical mixing and a cross frontal transport. These processes occur concomitantly with the most vigorous ocean–air heat loss (~ 70 TW just for BS) of the Arctic (Serreze et al., 2007; Smedsrud et al., 2010), which favors the winter Barents Sea Waters production. Only a few studies (e.g. Parson et al., 1996) provide local descriptions of the polar front, which separates the Atlantic Waters from the Arctic Waters in the western part of the BS. To our

OSD
12, 449–492, 2015

knowledge, no detailed description of the frontal structure has been done in the eastern part of the BS.

The BS is the only Arctic Sea with sufficient available in-situ observations to perform reliable analysis of the interannual summer variability. We present in Sect. 2 the data we have gathered to produce a more comprehensive database than those previously used. A regional ocean circulation model (the SINMOD model, see Slagstad and McClimans, 2005) has also been used to complete the study of the variability. The following sections describe the mean hydrography of the BS, the mean position of the fronts and lastly the interannual variability and trend which can be identified in the BS.

2 Data and methods

2.1 Data

The International Council for the exploration of the Sea (ICES, http://ocean.ices.dk, see for example Nilsen et al., 2008) and the Arctic and Antarctic Research institute (AARI, Russia, Ivanov et al., 1996; Korablev et al., 2007) provide processed hydrographic data sets which document the BS area. We have merged these data sets to constitute a new database which now is likely the most complete hydrographic collection for the BS. This database contains more than 130 000 CTD profiles; it includes the BSO section (see Fig. 1a) (repeated 6 times a year, every two months) and the Vardø section (repeated twice a year, in winter and summer). The accuracy of the data is difficult to specify. On rare occasions, the poorest accuracy might be 0.1 °C in temperature and 0.1 in salinity. However, after interpolation by kriging (see just below), the data associated with estimation errors below 20 % allowed us to build summer time-series going from 1980 to 2011 for temperature and salinity.

OSD
12, 449–492, 2015

2.2 Kriging: an optimal method for interpolating data

Kriging is an interpolation technique which provides the Best Linear Unbiased Estimator of an unknown field (Journel and Huijbregts, 1978; Kitanidis, 1997). The originally sparsely sampled data are characterized by a semivariogram (or equivalently a covariance function) which depends only on the distance between measured sample points and represents their spatial correlation. This semivariogram is computed and then used to interpolate the data on a regular grid.

This technique first allowed us to derive temperature, salinity and density fields for each summer (August and September) from 1980 to 2011, on a grid whose resolution is 0.5° longitude × 0.25° latitude. For each variable, four fields have been computed: the first field depicts the surface, the second field depicts an upper layer between 0 and 50 m (the high frequency variability is important in this layer and consequently the data are difficult to exploit), the third field depicts a mid-depth layer between 50 and 100 m (the vertical variations of the temperature and salinity are generally smaller than in the upper layer, and the low frequency variability easy to detect), and the fourth field depicts a bottom, nearly homogeneous layer between 100 and 200 m. In order to have almost 100 % of the BS surface covered by the data set, the study area has been limited to the area shown in Fig. 1a (70–80° N, 10–65° E). Data coverage is less dense on the eastern part of the domain (Fig. 2) because the observations became sparser in the Russian part of the BS during the last decade. However, this does not seem to have an impact on the results shown below.

The same technique was used to interpolate the temperature and salinity fields coming from the Vardø section. The resolution of the (vertical) grid is 0.125° latitude × 5 m depth.

2.3 SINMOD 3-D model description and set-up (Slagstad, 1987)

SINMOD (SINtef Ocean MODel) is a coupled 3-D hydrodynamic chemical and biological model system that has been developed and used for more than 25 years at SINTEF

OSD
12, 449–492, 2015

(Scientist and Industrial Research Foundation, Norway). The hydrodynamic part of the model is based on the primitive equations which are solved by finite differences using an Arakawa C-grid (Mesinger and Arakawa, 1976). The model uses z coordinates in the vertical direction. The ice model is based on the elastic-viscous-plastic rheology (see Hunke and Dukowicz, 1997). The model is forced by transports through open boundaries (Slagstad and Wassmann, 1996), atmospheric fluxes provided by the European Centre for Medium-Range Weather Forecasts (ECMWF) reanalysis data (ERAi), freshwater input and tides. The four tidal components (M2, S2, K1 and N2) are imposed by specifying the transports at the open boundaries of the large-scale model. Data are taken from TPXO 6.2 (http://polaris.esr.org/ptm_index.html). Freshwater run-off, river discharge and run-off from land are based on outputs obtained from a simulation with a hydrological model (Dankers and Middelkoop, 2007). The model has been validated from in-situ current measurements and temperature fields, and physical and chemical observations made at the Vardø section. More details about the model and its validation can be found in Slagstad et al. (1999) and Slagstad and McClimans (2005).

For this study, we use monthly temperature and salinity fields obtained from SINMOD runs performed for the 1979–2012 period over the whole Arctic with a 20 km grid resolution and 25 levels. Initial values of temperature and salinity were taken from the 1998 NODC World Ocean Atlas built by the NOAA-CIRES Climate Diagnostics Center, Boulder, Colorado, USA (http://www.cdc.noaa.gov/) to perform this experiment. We also use for the 1997–2001 period a high resolution (4 km and 34 levels) numerical experiment performed with the same model on a reduced domain covering the BS.

The low resolution experiments are used to analyze the process leading to the observed variability of the temperature and salinity fields during the 1980–2011 period. The high resolution experiment allowed us to study the changes experienced by the fronts between a cold and a warm period. In order to remove the "noise" due to the eddy activity, a Gaussian filter with a standard deviation of 36 km has been applied to the temperature and salinity fields.

OSD
12, 449–492, 2015

3 Summer climatology of the water masses from the observations

3.1 Water masses

The Θ–S diagram of the Gimsoy transect in the Norwegian Sea (shown in Fig. 3a for the 1980–1985 period) allows us to identify the summer Atlantic Water (AW, depth ~ 200 m, $T \sim 7\,^{\circ}$C, $S \sim 35.25$) and the summer Norwegian Coastal Current Water (NCCW, depth ~ 50 m, $T > 6\,^{\circ}$C, $S < 34.4$), which both enter the BS. Note that the Norwegian Coastal Current Waters (NCCW) has a large temperature and salinity seasonal variability: the temperature can reach more than 12 °C at the surface in summer and the salinity ranges from 32 to 34.4. The intermediate Arctic Water ($T \sim -1\,^{\circ}$C, $S \sim 34.9$) is found at a depth of around 1200 m and consequently cannot enter the BS.

North of 80° N, in the Nansen Basin, from surface down to about 100 m, one finds the Arctic Water which can penetrate the BS. It clearly appears in the Θ–S diagram of Fig. 3b ($T < 0\,^{\circ}$C, $S < 34.7$).

The Atlantic Waters, Norwegian Coastal Current Waters, and Arctic Waters we have just introduced are thus found in the BS, with slightly modified characteristics. Barents Sea Water (BSW) and Fresh Water (FW) have a more local origin. Table 1 summarizes the characteristics of these five water masses for the BS; the given values are based on the ones generally found in literature. The square domains represented in the Θ–S diagrams in Fig. 4 have been built from these values.

These figures illustrate the large differences both in salinity and temperature of the water masses of the BS. The Barents Sea Waters (also called "Barents Sea Atlantic derived water", "modified Atlantic Water" or "Polar Front Water") is formed on the BS shallow banks (Central Bank), mainly in winter, by the mixing of the other water masses and by large heat losses. For example, the temperature of the Atlantic Waters is about 6 °C at BSO, which agrees with Årthun and Schrum (2010), whereas that of the Barents Sea Waters is about 0 °C between Nova Zemlya and Franz Josef Land (Gammelsrød et al., 2009). The Barents Sea Waters then cascades down the deeper regions (Årthun et al., 2011) and the largest part finally flows out of the BS toward the Arctic Ocean

OSD
12, 449–492, 2015
The Barents Sea polar front and water masses variability (1980–2011)
L. Oziel et al.

to form the Intermediate Arctic Water (Rudels et al., 1994). The Barents Sea Waters has a high density, often greater than 1028 kg m^{-3}. The densest Barents Sea Waters (not shown) is found east of the Vardø section, and has nearly the same hydrographic properties as the Intermediate Arctic Water found at around 1200 m depth, outside the BS (see Fig. 3).

The Barents Sea Waters scarcely appears in the BSO section (Fig. 4a) and becomes more visible in the Vardø section (Fig. 4b). This agrees with the results illustrated in Fig. 5, which characterizes the horizontal occurrence of water masses in August–September in the BS for the period 1980–2011. Only the layer between 50 and 100 m has been considered for this computation (see Sect. 2). A percentage of 100 % indicates that the water mass is present every summer in the concerned area. The Atlantic Waters is always present in the south-west BS, the BSO trough and up to the Great Bank (Fig. 5a), and sometimes spreads further north and east in the deepest part of the BS such as the central basin (occurrence of about 20–30 % in these areas). The Arctic Waters occurrence (Fig. 5b) is close to 100 % in the North-West BS and over the Spitzbergen bank. The locally formed Barents Sea Waters (Fig. 5c) mainly resides over the Central Bank and in the Central Basin as expected (Årthun et al., 2011), but also in the eastern part of the BS. The Norwegian Coastal Current Waters (Fig. 5d) has a significant contribution in the southern part of the BS accounting for about one third of the inflowing waters through BSO. It remains near the coast, west of 30° E, then spreads up to 74° N with other waters from the White Sea, Pechora Sea, Kara Sea and rivers.

In the eastern part of the BS, the occurrence of a particular water mass is sometimes lower than 30 %, and no water mass is dominating east of 40° E. The shallow coastal area (depth shallower than 200 m) of the eastern BS is influenced by the four main water masses, i.e. the Atlantic Waters, Arctic Waters, Barents Sea Waters, and Norwegian Coastal Current Waters. This suggests that these different water masses can easily mix in this area. There is also a large contribution of ice in the fresh surface layer (not shown). Lastly, the dynamic of the BS is less constrained by the topography in the

OSD
12, 449–492, 2015

eastern part of the BS than in the western part (Parson et al., 1996; Johannessen and Foster, 1978; Gawarkiewicz and Plueddemann, 1995). Consequently, the limits of the domains where the water masses are present no longer follow the isobaths.

3.2 Transformation of the water masses between BSO and Vardø

The temperature and salinity at the BSO and Vardø sections (Fig. 4) allow us to describe the transformations of the water masses during their path in the BS in a more precise way. To carry this out, we define "ideal water masses" which exemplify the specific properties of each water mass:

- Ideal Arctic Water (blue dot in Fig. 4) is defined by a minimum of temperature since it is the coldest BS water mass.
- Ideal Barents Sea Water (black dot in Fig. 4) is defined by a maximum of density since it is the densest BS water mass.
- Ideal Atlantic Water (red dot in Figs. 3a and 4) is defined by a maximum of salinity since it is the most saline BS water mass.

An ideal Norwegian Coastal Current Water was not defined because the points which characterize it are too scattered. The Norwegian Coastal Current Waters indeed depend on many external forcings (freshwaters inputs, solar heating, etc).

As it progresses from Gimsoy to BSO, the ideal Atlantic Water experiences a weak decrease in salinity (of about 0.06) and a negligible decrease in temperature. This decrease is easily explained by a mixing with the fresher Norwegian Coastal Current Waters facilitated by the strong eddy activity. The transformations are greater between BSO and Vardø: the salinity of the ideal Atlantic Water loses about 0.01 and the temperature more than 2 °C. They are caused by a mixing with the adjacent Barents Sea Waters and Arctic Waters and chiefly by the strong sensible heat fluxes which cool the surface water in winter, inducing a significant drop of the temperature of the Atlantic

OSD
12, 449–492, 2015

Waters in the western part of the basin. Note, however, that seasonal variations of Atlantic Waters at Vardø remain small and no seasonal variability is found for the Barents Sea Waters (not shown).

3.3 Fronts in the Barents Sea

The front which separates the Atlantic Waters from the Arctic Waters in the Barents Sea is denoted as the polar front. It follows the bottom topography in the western part and consequently remains stable from one year to the other. Its position is less clear in the eastern part and the new database presented in Sect. 2 can help clarify this. We thus computed the position of the fronts which separate the Atlantic Waters, the Arctic Waters and also the Barents Sea Waters. Indeed, the latter naturally appears when an objective interpolation method is employed.

The computation has been done for the summer data, between 50 and 100 m (see Sect. 2), where the Atlantic Waters is easily found. This allows us to eliminate the surface layer where temperature and salinity strongly vary (of about 1.0–3.0 °C and 0.2–0.8) and to avoid the freshwater coming from the Pechora and White Seas in the eastern BS or from the melting ice. Below 100 m, the vertical mixing due to the turbulence generated by the tidal flow is strong (Parson et al., 1996) and the effects of salinity on the density compensate those of temperature. The existence of the fronts thus becomes more elusive because the density gradients vanish.

Figure 6a and d respectively shows the mean temperature and salinity fields obtained from the data described in Sect. 2 between 50 and 100 m (August–September of the 1980–2011 period). The temperature of the Atlantic Waters in the south-western part of the basin exceeds 7 °C whereas that of the Arctic Waters is below −1 °C in the North. The salinity ranges from less than 34 for the Norwegian Coastal Current Waters close to the Norwegian coasts and for the Arctic Waters in the northern part of the basin, and to more than 35 for the core of the Atlantic Waters which enters through the BSO. The temperature and salinity fronts are easy to discern in the western part of the basin in these figures, yet it is more difficult in the eastern part. Consequently, we have developed an algorithm which allows to determine the position of the fronts in a more objective way.

This algorithm is based on the computation of Probability Density Functions (PDF). We present it for the temperature field. First, the points where the norm of the temperature gradient exceeds 0.1 $^{\circ}$C km^{-1} are selected. The histogram of the temperature T of these points is built, representing the number of points for which this temperature is in the interval $T-\mathrm{d}T$ and $T+\mathrm{d}T$ with $\mathrm{d}T = 0.05\,^{\circ}$C, where T represents the range of possible temperatures (see Fig. 6b). The PDF is obtained by dividing this number by the total number of points. The maximum of the PDF is determined, and the corresponding temperature of $T_{\mathrm{m}} = 0.8\,^{\circ}$C is determined. At last, the standard deviation SD is computed as: SD = 2.4 $^{\circ}$C. The frontal zone is defined by the area delimited by the isotherms $T_{\mathrm{m}} - \mathrm{SD}/2 = -0.4\,^{\circ}$C and $T_{\mathrm{m}} + \mathrm{SD}/2 = 2\,^{\circ}$C. It is represented in Fig. 6a and c where the three isotherms (red lines) have been drawn. The area limited by the two extreme isotherms is the one where it is the most probable to find a temperature gradient exceeding the initial threshold 0.1 $^{\circ}$C km^{-1}. The method is robust. The results do not significantly change when the threshold value for the gradient is reasonably modified (for example when 0.10 $^{\circ}$C km^{-1} is replaced by 0.08 or 0.12 $^{\circ}$C km^{-1}).

The same method was used for the salinity, with a threshold value equal to 0.01 km^{-1}, resulting in the PDF curve shown in Fig. 6e. The frontal area is then delimited by the isohalines $S = 34.45$ and $S = 34.75$ (mid value: 34.6). It is represented in Figs. 6d and 5e where the three isohalines (blue lines) have been drawn.

In the western part of the BS, the frontal areas computed from the temperature or salinity fields are narrow, nearly joined, associated with strong gradients (see Figs. 6c and 5e), and follow the bottom topography as expected. The situation is more complicated east of the Vardø section. Two frontal areas clearly appear: a northern one associated with the salinity gradients (of about 0.004 km^{-1}; see Fig. 6f), and a southern one associated with the temperature gradients (of about 0.05 $^{\circ}$C km^{-1}; see Fig. 6c). To distinguish them, we denoted the first one the “North Polar Front” and the second one the “South Polar Front”. They are partly linked to the bottom topography: the “North Po-

OSD
12, 449–492, 2015

lar Front" heads north, up to the 79° N latitude and the SPF heads south, crossing over the Central Bank, up to the Central Basin. Note that the 2 °C isotherm which shows the southernmost position of the "South Polar Front" (see Fig. 6c) is located further south than the front defined by Harris et al. (1998) in the eastern BS.

This description is compatible with the results of the previous subsection and those found in literature (see for example Parson et al., 1996 or Harris et al., 1998).

It is clear from Fig. 7 that the front at about 74° N is dominated by the temperature gradient. The situation is more complex for the other fronts. Consequently, to evaluate the impact of the temperature and salinity gradients on the density gradients, we have computed the dimensionless horizontal density ratio D_x defined by Rudnick and Ferrari (1999):

$$D_x = \alpha \cdot T_x / \beta \cdot S_x$$

(where α is the thermal expansion coefficient of the seawater, β is the haline contraction coefficient, T_x and S_x are horizontal temperature and salinity gradients in °C m^{-1} and m^{-1} respectively shown in Fig. 7c and d). The result of this computation is shown in Fig. 7e: the "Norwegian Coastal Current Front" and the "North Polar Front" are dominated by the effects of salinity ($D_x < 1$; blue) whereas the "South Polar Front" is dominated by those of the temperature ($D_x > 1$; red).

4 Variability of the water masses of the Barents Sea

The Arctic Oscillation index (AO, see Fig. 8a), is defined as the pressure difference between the North Pole and the eastern Atlantic at 20° N and according to Thompson and Wallace (1998) it was the dominant pattern of the atmospheric interannual and decadal variability over the Arctic. When this index is low, the atmospheric circulation becomes more anticyclonic and the air temperature decreases over the eastern Arctic. Consequently, the heat fluxes between the atmosphere and ocean are enhanced, particularly in winter. Furthermore, the westerlies are enhanced and advect more Atlantic

OSD
12, 449–492, 2015

Waters into the BS from the Norwegian Sea through the BSO. The consequences of these changes are well marked in the BS. For example, the maximum extent of the sea ice (Fig. 8b, see also Furevik, 2001), which is a good indicator of the climate in the BS area (Serreze et al., 2007) is significantly correlated with the AO index (the correlation is about −0.33). As expected, a maximum of the sea ice extent is generally associated with a low AO index, as shown in Fig. 8 by the vertical blue bands enhancing the correlations. Similarly, the correlation between the winter (March) sea surface temperature (SST) or air temperature at 2 m (T2) in the BS (Fig. 8c) and the AO index is significant, of about 0.36 and 0.23 respectively (the anti-correlations between the winter SST or T2 and the maximum extent of sea ice both reach −0.55).

In addition to this non seasonal variability, the BS has experienced remarkable climate changes for the last decades. For example, the maximum sea ice extent (Fig. 8b) has decreased by about 200 000 km^2 between 1980 and 2011, the T2 (Fig. 8c) has increased by about 2 °C and the heat losses of the ocean have been reduced by about $-50\,W\,m^{-2}$ (Fig. 9c).

To detect the links between the interannual variability of the atmosphere and that of the water masses in the BS, a yearly index has been defined for each water mass, equal to the relative volume that a water mass occupies. This relative volume is obtained by adding the volumes of each grid cell where a water mass is present and dividing the result by the volume of all the grid cells. The computation based on the database of Sect. 2 has been done between 0 and 200 m depth. The corresponding series for the Atlantic Waters and Arctic Waters indexes are shown in Fig. 9a. The correlation between the AO index and the Atlantic Waters or the Arctic Waters index is not significant, however the correlation between the Atlantic Waters (resp. Arctic Waters) and the winter ice cover reaches −0.30 (resp. 0.42) and is significant. Indeed, when the winter ice cover is low, the Atlantic Waters index is generally high and the Arctic Waters index low (for example in 1983–1984, 1990–1991, 2000, and 2007). The Atlantic Waters and Arctic Waters are strongly anti-correlated (correlation of about −0.75). The reverse occurs when the ice cover is high.

OSD
12, 449–492, 2015

The climate change observed in the atmosphere in the BS area is also clear in the ocean data. The Atlantic Waters index (resp. Arctic Waters index) shown in Fig. 9a presents a trend over the last 30 years, with perhaps an amplification during the last decade. The volume occupied by the Atlantic Waters (Arctic Waters) is about twice as large (as small) at the end of the series than at the beginning. This is compatible with the recent sea ice loss caused by an "Atlantification" of the BS due not only to an increase of Atlantic Waters temperature and salinity characteristics as described by Årthun et al. (2012) but to the increase of the Atlantic Waters volume present in the BS. According to Årthun et al. (2012), "Atlantification" meant the strengthening and warming of the Atlantic inflow that was observed both in observations and model simulations. This effect induced an increase of the heat transport, then a decrease of the sea ice extent. Here, we characterized the "Atlantification" by the large volume increase of the Atlantic Waters in the BS, which was not investigated in Årthun et al. (2012). This Atlantic Waters volume increase in the BS represents a major result of our study.

The processes leading to the "Atlantification" of the BS can be guessed from the analysis of the Gimsoy, BSO and Vardø sections. The ideal Atlantic Water (see the definition is Sect. 3) at Gimsoy section (Fig. 10a) experiences an increase of about +1 °C in temperature and +0.05 in salinity during the last thirty years. An increase is also observed at BSO and Vardø sections with +0.2 °C/+0.05 (Fig. 10b) and +1 °C/+0.02 (Fig. 10c) respectively. These changes are represented by the red lines in Fig. 10. The changes at BSO are perhaps made more visible in Fig. 11, which shows the series of the mean temperature and salinity between 1980 and 2011. The mean has been computed from the database between 50 and 200 m. A trend of about +1 °C and +0.2 is found on these series. These values are compatible with those found at Gimsoy section for the ideal Atlantic Water. At the Vardø section, the temperature and salinity of the ideal Barents Sea Water remain nearly constant and no changes have been detected on the Arctic waters.

These figures suggest that the hydrographical changes in the BS are driven by the inflow of Atlantic Waters which has become warmer in recent years. These warmer

OSD
12, 449–492, 2015
The Barents Sea polar front and water masses variability (1980–2011)
L. Oziel et al.

waters, coming from the Norwegian Sea, invade the BS and could prevent or slow down the formation of Barents Sea Waters. This increase of Atlantic Waters temperature is accompanied by an increase of Atlantic Waters volume transport according to Årthun et al. (2012).

The results based on the observations are mainly obtained from summer data, and thus ignore the hydrological conditions during the largest part of the year. This may be problematic since the Barents Sea Waters being formed in winter, their volume depends on winter conditions. Hence using numerical models, even though they show biases, may help completing the information given by the observations and possibly reveal when and where observations are missing.

The SINMOD model, as any model, (with a 20 km resolution, see Sect. 2) presents some biases: as an example, it overestimates the temperature by about 1 °C for the first 12 years between 1980 and 1992 and underestimates salinity by about −0.1 (especially during recent years) along the BSO (Fig. 11). Similar biases are found along the other sections. More globally, the mixed layer is slightly too deep, the deep waters are too homogeneous and the Barents Sea Waters is slightly too fresh and cold in comparison with the observations (fresher and colder). However, the winter mechanism of the Barents Sea Waters production is correctly represented (not shown) and the density is close to the observed density of the Barents Sea Waters. But, the model is unable to reproduce the trend that we found in the observations. Such biases are not unusual for models and the causes of these flaws are numerous (see for example Sundfjord et al., 2007, or Ellingsen et al., 2009). Despite these imperfections, the model correctly reproduces the observed BS seasonal cycle (not shown) and succeeds in capturing the interannual variability.

To characterize the interannual variability, water mass indexes have been computed for the SINMOD model, as it has been done for the observations (Fig. 9a). The correlation between the AO (Fig. 8a) and the Atlantic Waters (Arctic Waters) index of the model (Fig. 9b) is equal to 0.42 (−0.23). The correlation between the ice cover and the Atlantic Waters (Arctic Waters) index of the model is also significant and equal to

OSD
12, 449–492, 2015

−0.42 (0.74). As for the observations, the Atlantic Waters and Arctic Waters index series are strongly anti-correlated (the correlation is about −0.50). These changes can be associated with the variations of the winter net heat flux over the BS (see Fig. 9c; the correlation with the Atlantic Waters index series reaches −0.46). This suggest that local mechanisms are important: the interannual changes observed on the Atlantic Waters are not only due to remote changes which could occur upstream, for example in the Norwegian Sea.

The model results, which take into account the temperature and salinity values in winter, partly agree with the results obtained from the summer observations, as the water mass variations in the BS are significantly correlated with the sea ice extent. However they differ concerning the AO. Significant correlations between the AO and the Atlantic Waters or the Arctic Waters indexes are found in the model but not in the observations (though the ice extent is related to the principal mode of variability of the atmosphere over the Arctic). This discrepancy could be due to the fact that we only consider summer data in the study based on the observations.

At last, the model permits to analyze how well the Barents Sea Waters (Fig. 12) are produced. The largest heat losses of the ocean occur when the differences between the winter air and sea surface temperature are maximum (> 15 °C) and the ice cover is minimum (500 000 km^2). They can reach up to −200 or −300 W m^{-2} (see Fig. 8c). At that time the freshwater amount is generally maximum since the ice has melted and consequently the Barents Sea Waters volume is small. Indeed, the water column is more stratified and the convection reduced and the Barents Sea Waters formation inhibited. These conditions favors the formation of sea ice as illustrated in Fig. 8b (and can be viewed as a negative feedback). This induces the reject of a large amount of salt, which in turn favors the formation of denser waters and consequently the Barents Sea Waters formation. This mechanism is supported by the well-marked periodicity of the Barents Sea Waters index time series (with a dominant period of about 5–6 years) and the large anti-correlation coefficients between the Barents Sea Waters index time-series and the heat loss (−0.65) or the freshwater amount (−0.82).

OSD
12, 449–492, 2015

5 Variability of the fronts: a model study

The observations are too sparse – in particular in the eastern part of the BS – to study the variability of the fronts. Consequently, we used the high resolution SINMOD model (see Sect. 2) to determine how a change in the climate conditions over the BS could affect the position of the SPF and NPF (see Sect. 3). To do this, the model has been integrated from 1998 to 2000 and its results analysed.

In winter 1998, the AO index was negative and the ice covered more than 750 000 km^2 of the BS. The mean air temperature was lower than −6 °C. From 1998 to 2000, this situation has dramatically changed: the AO index became positive, the extent of the sea ice decreased of about 300 000 km^2, the air temperature increased of about 6 °C, the mean SST of 0.5 °C, and the mean temperature across BSO of 1 °C (Fig. 8). Meanwhile, the volume occupied by the Atlantic Waters increased (the Atlantic Waters index increased from 25 to 30 %). The contrast between 1998 and 2000 therefore allows us to investigate how the "South Polar Front" and "North Polar Front" could shift if the climate keeps on warming and the "Atlantification" of the BS continues.

The high resolution numerical model (4 km resolution) presents biases quite similar to the low resolution one. The temperature (salinity) is about 1.5 °C (0.15) too high in comparison with the observations, the differences reaching 2.0 °C (0.25) in the eastern part of the basin. The model underestimates the mean volume of Atlantic Waters but is able to represent its variability, as the Atlantic Waters index increases of about 3 % (from 17 to 20 %), which seems acceptable, considering the short period of time (three years) which is analysed. The model also predicts a decrease of the Arctic Waters index from 23 to 20 %, which seems compatible with the increase of Atlantic Waters.

The technique used to compute the position of the fronts from the observations has been applied for the model results. The PDFs have been computed in summer and winter 1998 and 2000 for temperature (Fig. 13) and salinity (Fig. 14). The corresponding position of the fronts is shown in Fig. 15. The "North Polar Front" is associated with the isohalines 34.7 in 1998 and 34.84 in 2000; the "South Polar Front" is associated with the isotherms 1.4 °C in winter 1998, 3.4 °C in summer 1998, 1.9 °C in winter 2000, and 4.1 °C in summer 2000. The seasonal variability of the fronts (represented by the red and blue lines in Fig. 15) remains weak, even though the salinity gradients are more pronounced during winter: the former, associated with the "North Polar Front", increases from 0.04 to 0.055 km^{-1}, The temperature gradients are stronger in summer and the latter, associated with the southern part of the "South Polar Front", increase from 0.3 to 0.4 °C km^{-1} (not shown).

The interannual variability of the "North Polar Front" is also negligible, though the climate conditions have changed. On the contrary, the position of the "South Polar Front" is considerably modified, shifting eastwards and northwards, turning around the Central Basin, and following the 200 and 300 m isobaths. The temperature gradient then exceeds 0.06 °C km^{-1} around the Novaya Zemlya Bank. This shift obviously accompanies the increase of the Atlantic Waters volume in 2000.

This high resolution numerical experiment therefore suggests that the "Atlantification" of the BS observed during the last decade could induce a northward shift of the "South Polar Front". In the model, the geographical area where the Barents Sea Waters are found should then be located further north. As the volume of the Barents Sea Waters remains unchanged, a northward shift of the modelled "North Polar Front" should be expected. This expected shift is not found in the numerical experiment. The unperfected representation of the Barents Sea Waters, whose temperature and salinity characteristics show some defaults in the model, and the idealized character of the experiment can explain this discrepancy between observations and model.

6 Discussion and conclusion

The results presented in this study have been obtained from a new extensive hydrographic database which is one of the most complete ones at the present time for this region. We built this database by merging the existing data sets with recent Russian data documenting the eastern BS.

OSD
12, 449–492, 2015

Årthun et al. (2011) defined the "Atlantification" process as an increase of the Atlantic inflow towards the Barents Sea and analyzed its consequences on the sea ice extent. The new database revealed the "Atlantification" had also significant consequences in the whole BS during the last 30 years related to a doubling of the Atlantic Waters volume. A saltier and warmer inflowing Atlantic Water was observed from the Gimsoy section in the Norwegian Sea, up to the Vardø section in the central BS. Consequently, the domain occupied by the Atlantic Waters extended further East and North. This especially affected the Eastern BS at the expense of the Arctic Waters that drastically decreased during the last decade as already observed by Lind et al. (2012). This trend was accompanied by a spectacular increase of the air temperature (Levitus et al., 2009). The last decade was the warmest of the last century (Boitsov et al., 2012) and is also characterized by the largest decrease of the sea ice extent in the BS ever observed (Cavalieri and Parkinson, 2012).

In the western part of the BS, the position of the polar front is constrained by the topography, following the Spitzbergen bank and the Great bank slopes. East of the Vardø section, the polar front splits into two branches, the so-called "South Polar Front" and "North Polar Front". The "South Polar Front" is dominated by the temperature gradients and is collocated with the 0.8 °C (±1.2 °C) isotherm; the "North Polar Front" is dominated by the salinity gradients and is collocated with the 34.6 (±0.15) isohaline. The Barents Sea Waters is formed between these two fronts by mixing of the Atlantic Waters with the Arctic Waters and cooling. Its properties are close to those of the Intermediate Waters found in the Nansen Basin as shown by Rudels et al. (1994). The eastern part of the BS is thus of first importance because it is the "mixing zone" where the dense Barents Sea Waters formation takes place.

The interannual variability is also visible in the oceanic data. Cold (1981–1982, 1987–1988, 1994, 1998, 2003–2004, and 2010) and warm (1984, 1990–1992, 1995, 2000–2001, and 2007–2008) periods have been documented by Furevik et al. (2001) and Adlandsvik and Loeng (1991). Cold and warm events appeared clearly by looking at the variability of the sea ice extent which is a good indicator of climate changes (Ser-

OSD
12, 449–492, 2015

reze et al., 2007). The sea ice extent variability was characterized by a period of about 5–7 years. We found that the variability of the Atlantic Waters volume is significantly correlated with that of the sea ice extent: a maximum of the Atlantic Waters volume generally corresponds to a minimum of the sea ice cover. The reverse is found for the Arctic Waters. The causes of these variations are difficult to determine because of the complexity of the ocean–ice–atmosphere system in the BS; this complexity has been discussed (Karcher et al., 2003; Ingvaldsen et al., 2003; Dickson et al., 2000; Sando et al., 2010 and Årthun et al., 2012). The variations of the Atlantic Waters inflow into the BS, which show cycles with a period of about 7–10 years (Bengtsson et al., 2004), could explain the variations of the Atlantic Waters volume in the BS. The direct forcing by the atmosphere has probably also an impact on the Atlantic Waters volume occupation in the BS but it is difficult to determine its role since it could also explain the variability of the Atlantic Waters inflow (Ingvaldsen et al., 2002). Lastly, Arctic Waters are clearly related to the ice cover.

The number of observed data is satisfactory enough to extract pertinent scientific information only during summer. In consequence, the analysis of in-situ observations have been done for August–September only. The use of the SINMOD model has allowed to examine what occurs in winter. As the model represents reasonably well the interannual variability, this study was relevant. However, we found that the Atlantic Waters and Arctic Waters variability is significantly correlated with the AO index in the model, which contrasts with the observations. This might suggest that our data analysis based on observations should be extended to winter data, even though the latter are scarce, to verify whether this contrasts would decrease. This would mean that global atmospheric changes over the Arctic could have a local impact in the BS.

The variability of the fronts is difficult to describe from the sole observations because they remain too scarce in the eastern part of the BS, where the topographic constraint becomes small, allowing large displacement of the fronts. A study, with the high resolution version of the SINMOD model, has thus been made to compare the situation between the year 1998 for which the winter ice cover was important and 2000 for which

OSD
12, 449–492, 2015

it was small. We found that the Atlantic Waters" volume slightly increased (by about 3 %) and the "South Polar Front" significantly shifted northward, while the "North Polar Front" remained stationary. This suggests that the process of "Atlantification" could lead to a substantial northward displacement of the "South Polar Front". The Barents Sea Waters would then move further north.

The north-eastern part of the BS is one of the regions of the Arctic that is the most affected by the sea ice extent decline. As the sea ice is on the path of the Atlantic Waters, it is suggested that the "Atlantification" of the BS could slow down the formation of sea ice in winter by bringing warmer water in larger quantities (higher Atlantic Waters volume), and thus participate in the shrinking of the sea ice cover. This particularly endangers the sea ice of Novaya Zemlya Bank, which is crucial for the dense water formation in this area (Ivanov et al., 2005; note that a quite similar phenomenon has been observed North of Svalbard by Lind and Ingvaldsen, 2012). The formation of dense Barents Sea Waters could then not occur.

The BS can be considered as a robust "ocean cooler" and acts like a buffer zone between the World Ocean and the Arctic Ocean (Smedsrud et al., 2013). But at a time of drastic climate change, the ocean–atmosphere–ice system of the BS experiences important modifications. Our study suggests that the eastern part of the BS is the most affected region: Atlantic Waters used to invade this area and displaced the "South Polar Front" northward. The long term response to these changes on the dense water formation in the BS, and therefore on the Arctic ventilation, remains unknown. Lastly, the BS accounting for 40 % of the primary productivity of the Arctic (Sakshaug, 2004), physical changes such as those we described and analyzed could also have significant impacts on the BS marine ecosystems (phytoplankton, carbon cycle and acidification).

Acknowledgements. The research leading to these results has received funding from the European Union under Grant Agreement no. 265863 within the Ocean of Tomorrow call of the European Commission Seventh Framework Programme. The EU project ACCESS is also funding the 3 year PhD of the lead author. The authors are particularly grateful to Michel Crépon for his many reviews. We also want to thank Xavier Capet for his help in the construction of the PDF method, and Michael Field for improvements on the final manuscript. The Hydrographic

data were provided by the ICES Data Centre (www.ices.dk) and the Arctic and Antarctic Research Institute, Russia. The SINMOD model is provided by Dag Slagstad from SINTEF fisheries in Trondheim, Norway. The ERA-Interim data were obtained from the European Centre for Medium-Range Weather Forecasts data server. Arctic Oscillation data were down-loaded from JISAO, Seattle, USA. Ice concentration were obtained from SSMI satellite, NSIDC, USA.

References

Aagaard, K. and Woodgate, R. A.: Some thoughts on the freezing and melting of sea ice and their effects on the ocean, Ocean Model., 3, 127–135, 2001.

Anderson, L. G., Jones, E. P., and Rudels, B.: Ventilation of the Arctic Ocean estimated by a plume entrainment model constrained by CFCs. J. Geophys. Res., 104, 13423–13429, 1999.

Årthun, M. and Schrum, C.: Ocean surface heat flux variability in the Barents Sea, J. Marine Syst., 83, 88–98, 2010.

Årthun, M., Ingvaldsen, R. B., Smedsrud, L. H., and Schrum, C.: Dense water formation and circulation in the Barents Sea, Deep-Sea Res. Pt. I, 58, 801–817, 2011.

Årthun, M., Eldevik, T., Smedsrud, L. H., Skagseth, Ø., and Ingvaldsen, R. B.: Quantifying the influence of Atlantic heat on Barents Sea ice variability and retreat, J. Climate, 25, 4736–4743, 2012.

Dankers, R. and Middelkoop, H.: River discharge and freshwater runoff to the Barents Sea under present and future climate conditions, Climatic Change, 87, 131–153, 2007.

Ellingsen, I., Slagstad, D., and Sundfjord, A.: Modification of water masses in the Barents Sea and its coupling to ice dynamics: a model study, Ocean Dynam., 59, 1095–1108, 2009.

Furevik, T.: Annual and interannual variability of Atlantic Water temperatures in the Norwegian and Barents Seas: 1980–1996, Deep-Sea Res. Pt. I, 48, 383–404, 2001.

Gammelsrød, T., Leikvin, Ø., Lien, V., Budgell, W. P., Loeng, H., and Maslowski, W.: Mass and heat transports in the NE Barents Sea: observations and models, J. Marine Syst., 75, 56–69, 2009.

Gascard, J., Raisbeck, G., Sequeira, S., Yiou, F., and Mork, K. A.: The Norwegian Atlantic Current in the Lofoten basin inferred from hydrological and tracer data (^{129}I) and

OSD
12, 449–492, 2015

The Barents Sea polar front and water masses variability (1980–2011)

L. Oziel et al.

its interaction with the Norwegian Coastal Current, Geophys. Res. Lett., 31, L01308, doi:10.1029/2003GL018303, 2004.
Gawarkiewicz, G. G. and Plueddemann, A. J.: Topographic control of thermohaline frontal structure in the Barents Sea Polar Front on the south flank of Spitsbergen Bank, J. Geophys. Res., 100, 4509–4524, 1995.
Harris, C. L., Plueddemann, A. J., and Gawarkiewicz, G. G.: Water mass distribution and polar front structure in the western Barents Sea, J. Geophys. Res., 103, 2905–2917, 1998.
Hunke, E. C. and Dukowicz, J. K.: An elastic–viscous–plastic model for sea ice dynamics, J. Phys. Oceanogr., 27, 1849–1867, 1997.
Ingvaldsen, R., Loeng, H., and Asplin, L.: Variability in the Atlantic inflow to the Barents Sea based on a one-year time series from moored current meters, Cont. Shelf Res., 22, 505–519, 2002.
Ingvaldsen, R., Loeng, H., Ottersen, G., and Ådlandsvik, B.: Climate variability in the Barents Sea during the 20th century with focus on the 1990s, ICES Marine Science Symposium, Edinburgh, 2003.
Ingvaldsen, R. B., Asplin, L., and Loeng, H.: Velocity field of the western entrance to the Barents Sea, J. Geophys. Res., 109, C03021, doi:10.1029/2003JC001811, 2004.
Inoue, J., Hori, M. E., and Takaya, K.: The role of Barents Sea Ice in the wintertime cyclone track and emergence of a warm-Arctic Cold-Siberian Anomaly, J. Climate, 25, 2561–2568, 2012.
Johannessen, O. M. and Foster, L. A.: A note on the topographically controlled Oceanic Polar Front in the Barents Sea, J. Geophys. Res., 83, 4567, doi:10.1029/JC083iC09p04567, 1978.
Karcher, M., Kulakov, M., Pivovarov, S., Schauer, U., Kauker, F., and Schlitzer, R.: Atlantic Water flow to the Kara Sea – comparing model results with observations, in: Siberian River Runoff in the Kara Sea: Characterisation, Quantification, Variability and Environmental Significance, edited by: Stein, R., Fahl, K., Fütterer, D. K., and Galimov, E., Proceedings in Marine Science, Elsevier, 47–69, 2003.
Loeng, H.: Features of the physical oceanographic conditions of the Barents Sea, Polar Res., 10, 5–18, in: Proceedings of the Pro Mare Symposium on Polar Marine Ecology, edited by: Sakshaug, E., Hopkins, C. C. E., and Britsland, N. A., 1991.
Martin, S. and Cavalieri, D. J.: Contributions of the Siberian shelf polynyas to the Arctic Ocean intermediate and deep water, J. Geophys. Res., 94, 12725–12738, 1989.

OSD
12, 449–492, 2015

The Barents Sea polar front and water masses variability (1980–2011)

L. Oziel et al.

Mesinger, F. and Arakawa, A.: Numerical methods used in atmospheric models, Global Atmospheric Research Programme – WMO-ICSU Joint Organizing Committee, 1, 1976.
Midttun, L. and Loeng, H.: Climatic variations in the Barents Sea. The effect of oceanographic conditions on distribution and population dynamic of commercial fish stocks in the Barents Sea, Proceeding of the third Soviet-Norwegian Symposium, Murmansk, 26–28 May 1986, 1987.
Nilsen, J. E. Ø., Hátún, H., Mork, K. A., and Valdimarson, H.: The NISE dataset, Tech. Rep. 07-01, Faroes Fish. Lab., Tórshavn, Faroe Islands, 2008.
Parsons, A. R., Bourke, R. H., Muench, R. D., Chiu, C.-S., Lynch, J. F., Miller, J. H., Plueddemann, A. J., and Pawlowicz, R.: The Barents Sea Polar Front in summer, J. Geophys. Res., 101, 14201–14221, doi:10.1029/96JC00119, 1996.
Pfirman, S. L., Bauch, D., and Gammelsrød, T.: The Northern Barents Sea: Water Mass Distribution and Modification, Geophysical Monograph 85, The Polar Oceans and their Role in Shaping the Global Environment, 1994.
Proshutinsky, A. Y. and Johnson, M. A.: Two circulation regimes of the wind-driven Arctic Ocean, J. Geophys. Res., 102, 12493–12514, 1997.
Rudels, B., Jones, E. P., Anderson, L. G., and Kattner, G.: On the Intermediate Depth Waters of the Arctic Ocean, Geophysical Monograph 85, The Polar Oceans and Their Role in Shaping the Global Environment, 1994.
Rudnick, D. L. and Ferrari, R.: Compensation of horizontal temperature and salinity gradients in the ocean mixed layer, Science, 283, 526–529, 1999.
Schauer, U., Muench, R. D., Rudels, B., and Timokhov, L.: Impact of eastern Arctic shelf waters on the Nansen Basin intermediate layers, J. Geophys. Res., 102, 3371–3382, 1997.
Schauer, U., Loeng, H., Rudels, B., Ozhigin, V. K., and Dieck, W.: Atlantic water flow through the Barents and Kara Seas, Deep-Sea Res. Pt. I, 49, 2281–2298, 2002.
Screen, J. A. and Simmonds, I.: The central role of diminishing sea ice in recent Arctic temperature amplification, Nature, 464, 1334–1337, 2010.
Serreze, M. C., Barrett, A. P., Slater, A. G., Woodgate, R. A., Aagaard, K., Lammers, R. B., Steele, M., Moritz, R., Meredith, M., and Lee, C. M.: The large-scale freshwater cycle of the Arctic, J. Geophys. Res., 111, C11010, doi:10.1029/2005JC003424, 2006.
Serreze, M. C., Holland, M. M., and Stroeve, J.: Perspectives on the Arctic's shrinking sea-ice cover, Science, 315, 1533–1536, 2007.

OSD
12, 449–492, 2015

Skagseth, Ø.: Recirculation of Atlantic Water in the western Barents Sea, Geophys. Res. Lett., 35, L11606, doi:10.1029/2008GL033785, 2008.
Slagstad, D. and Wassmann, P.: Climate Change and carbon flux in the Barents Sea: 3-D simulations of ice-distribution, primary production and vertical export of particulate organic carbon, Natl. Inst. Polar Res., 51, 119–141, 1996.
Slagstad, D., Downing, K., Carlotti, F., Hirche, H. J.: Modelling the carbon export and air–sea flux of CO_2 in the Greenland Sea, Deep-Sea Res. Pt. II, 46, 1511–1530, 1999.
Slagstad, D. and McClimans, T. A.: Modeling the ecosystem dynamics of the Barents sea including the marginal ice zone: I. Physical and chemical oceanography, J. Marine Syst., 58, 1–18, 2005.
Smedsrud, L. H., Ingvaldsen, R., Nilsen, J. E. Ø., and Skagseth, Ø.: Heat in the Barents Sea: transport, storage, and surface fluxes, Ocean Sci., 6, 219–234, doi:10.5194/os-6-219-2010, 2010.
Smedsrud, L. H., Essau, I., Ingvaldsen, R. B., Haugan, P. M., Li, C., Sien, V. S., Olsen, A., Omar, A. M., Otterå, O. H., Risebrobakken, B., Sandø, A. B., Semenov, V. A., and Sorokina, S. A.: The role of the Barents Sea in the Arctic climate system, Rev. Geophys., 51, 415–449, doi:10.1002/rog.20017, 2013.
Sundfjord, A., Fer, I., Kasajima, Y., and Svendsen, H.: Observations of turbulent mixing and hydrography in the marginal ice zone of the Barents Sea, J. Geophys. Res., 112, C05008, doi:10.1029/2006JC003524, 2007.
Thompson, D. W. J. and Wallace, J. M.: The Arctic oscillation signature in the wintertime geopotential height and temperature fields, Geophys. Res. Lett., 25, 1297–1300, 1998.

OSD
12, 449–492, 2015

Table 1. Water masses definitions for the Barents Sea.

Atlantic Waters (AW): $S > 34.8$, $T > 3\,^{\circ}\mathrm{C}$.
Arctic Waters (ArW): $S < 34.7$, $T < 0\,^{\circ}\mathrm{C}$.
Barents Sea Waters (BSW): $S > 34.8$, $T \leq 2\,^{\circ}\mathrm{C}$ ($\rho > 1027.8\,\mathrm{kg\,m^{-3}}$).
Norwegian Coastal Current Waters (NCCW): $S < 34.4$, $T > 3\,^{\circ}\mathrm{C}$.
Fresh Waters (FW): $S < 34.4$, $0 < T < 3\,^{\circ}\mathrm{C}$.

OSD
12, 449–492, 2015

Table A1. Glossary of acronyms.

AO:	Arctic Oscillation index
AW:	Atlantic Waters
ArW:	Arctic Waters
BS:	Barents Sea
BSO:	Barents Sea Opening (BS AW entrance section)
BSW:	Barents Sea Waters
FW:	Freshwaters
NCCF:	Norwegian Coastal Current Front
NCCW:	Norwegian Coastal Current Waters
NPF:	North Polar Front
SPF:	South Polar Front

OSD
12, 449–492, 2015

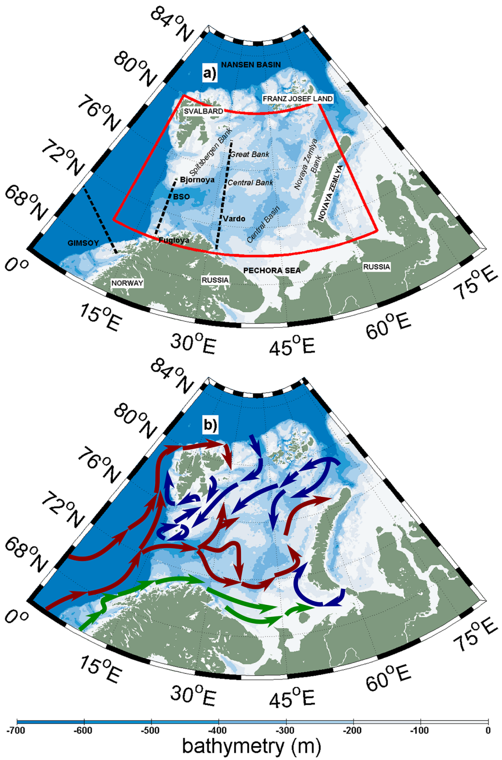

Figure 1. (a) Barents Sea map with bathymetry. The red line delimits the studied area. Repeated sections are represented in dashed black line: GIMSOY, BSO (Barents Sea Opening) and Vardø. **(b)** Schematic surface circulation of the main water masses (Atlantic water: red arrows; Arctic water: blue arrows: Norwegian Coastal Current: green arrows) (adapted from Harris et al., 1998).

OSD

12, 449–492, 2015

The Barents Sea polar front and water masses variability (1980–2011)

L. Oziel et al.

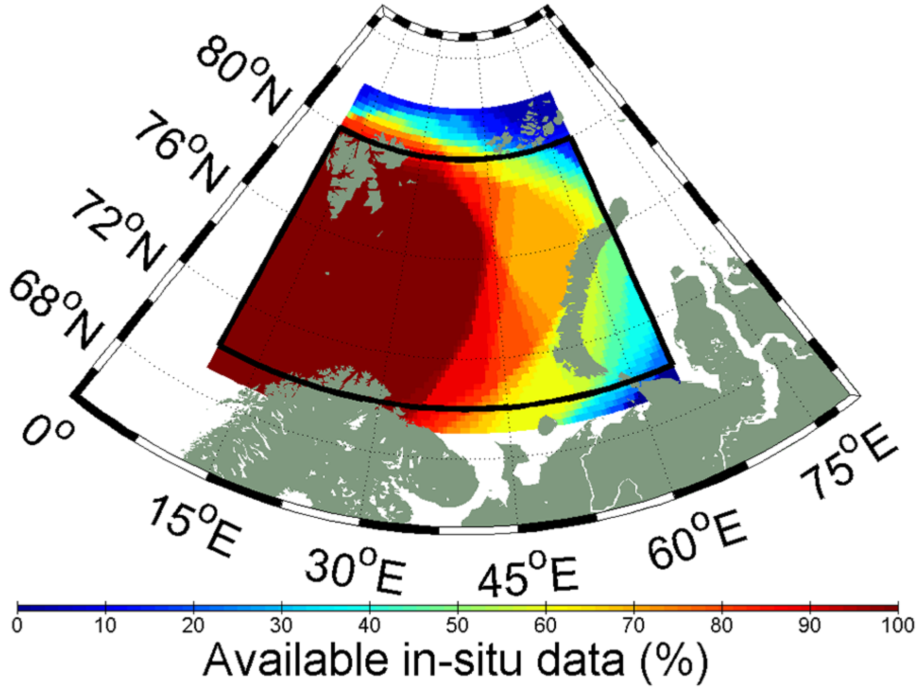

Figure 2. Available in-situ data: percentage of data for the 1980–2011 period.

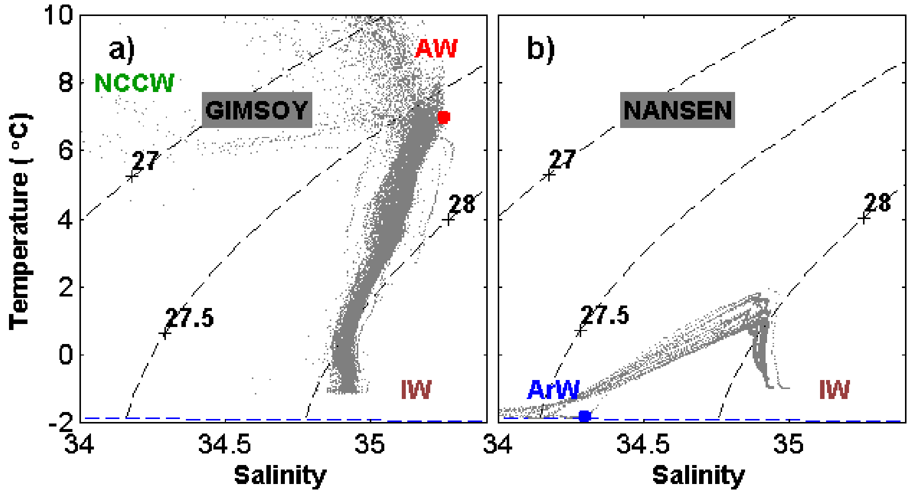

Figure 3. Potential temperature–salinity diagrams in August–September for the 1980–1985 period. **(a)** Gimsoy section **(b)** Nansen Bassin. Red dot: ideal Atlantic Water, blue dot: ideal Arctic Water. Intermediate Arctic Waters: IW.

OSD
12, 449–492, 2015

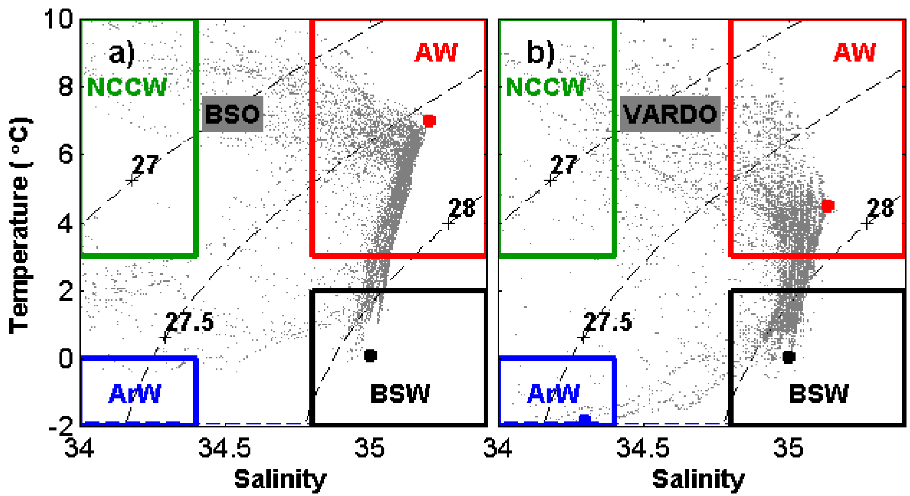

Figure 4. Potential temperature–salinity diagrams in August–September for the 1980–1985 period. **(a)** BSO section **(b)** Vardø section. Red dots: ideal Atlantic Water, black dots: ideal Barents Sea Water, and blue dots: ideal Arctic Water.

OSD
12, 449–492, 2015

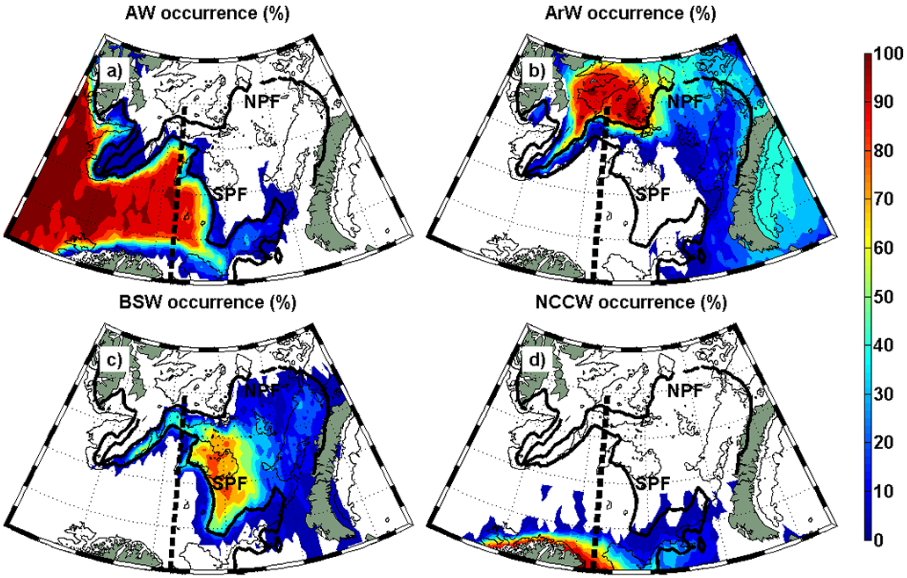

Figure 5. Water Mass Occurrences (%) over the 1980–2011 period in August–September for the 50–100 m layer. **(a)** Atlantic Water, **(b)** Arctic Water **(c)**, Barents Sea Water, **(d)** Norwegian Current Coastal Waters. The "South Polar Front" and "North Polar Front" (bold black lines), the Vardø section (dashed line), and the 200 m isobath (thin black line) are indicated.

OSD
12, 449–492, 2015

The Barents Sea polar front and water masses variability (1980–2011)

L. Oziel et al.

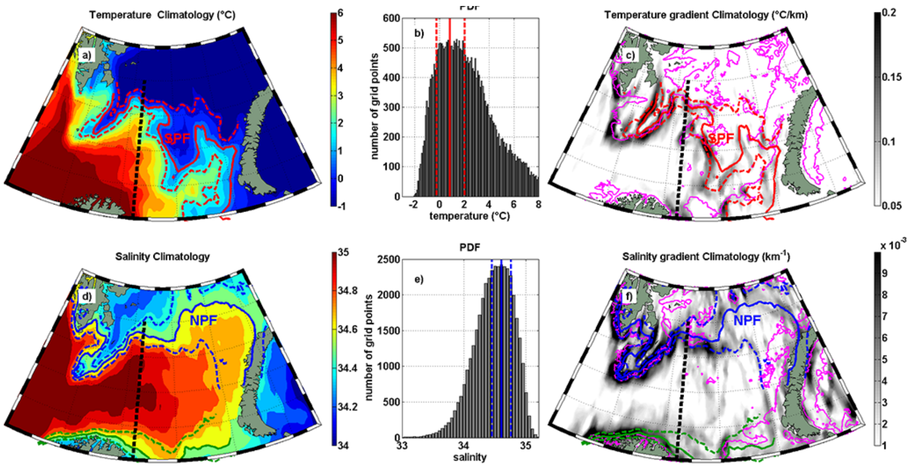

Figure 6. Temperature (°C) **(a)** and salinity **(d)** climatology for the 1980–2011 period (50–100 m layer, August–September). Probability Density functions (PDF) of the temperature and salinity fields are respectively shown in **(b)** and **(e)**. Horizontal gradients of temperature **(c)** and salinity **(f)**. The "Sotuh Polar Front" (SPF) (between the dashed red lines, +2 and −0.3 °C isotherms) and the "North Polar Front" (NPF) (between the dashed blue lines, 34.45 and 34.75 isohaline) are shown. Vardø section: black dashed line.

OSD
12, 449–492, 2015

The Barents Sea polar front and water masses variability (1980–2011)

L. Oziel et al.

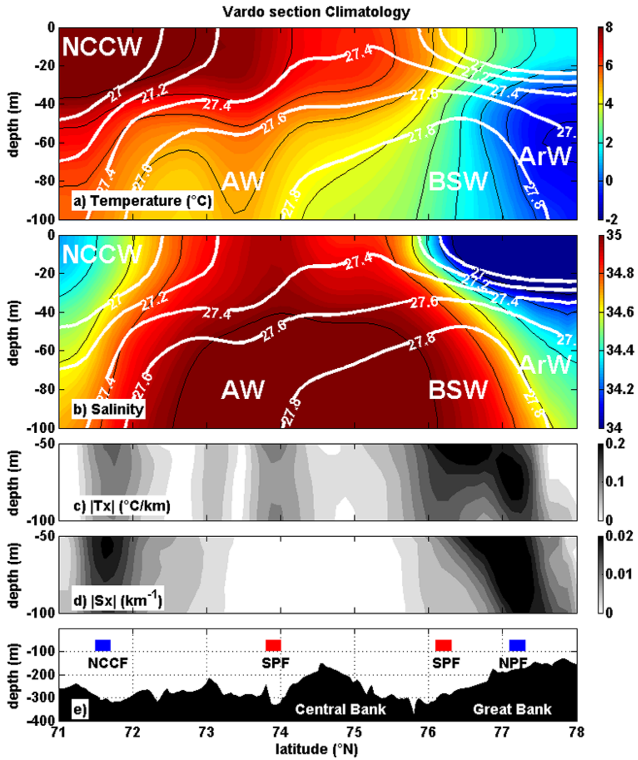

Figure 7. August–September climatology at Vardø section for the 1980–2011 period: temperature (°C) **(a)**, salinity **(b)**. White lines: isopycnes. Black lines: isotherms and isohalines (intervals: 1 °C and 0.1). Norms of horizontal temperature gradient **(c)** and salinity gradient **(d)**. Bathymetry **(e)**. The red and blue vertical patches respectively show which front is dominated by the temperature ($D_x > 1$) or salinity ($D_x < 1$) gradients.

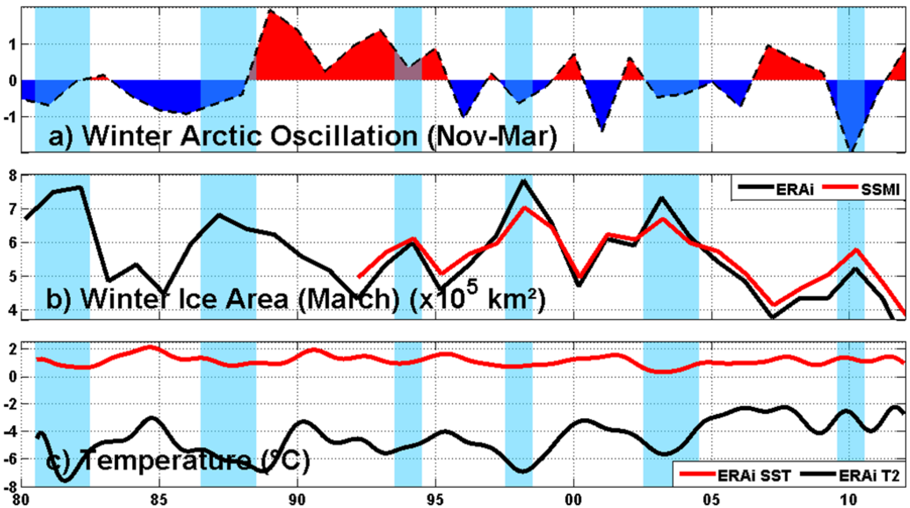

Figure 8. Inter-annual variations from 1980 to 2011 of: **(a)** winter Arctic Oscillation (November–March) from NOAA. **(b)** Maximum sea Ice extent (March). Black line: ERAi Re-analysis, red line: from SSMI. **(c)** Low-passed (14 months) air temperature at 2 m and SST from ERAi Re-analysis.

OSD
12, 449–492, 2015

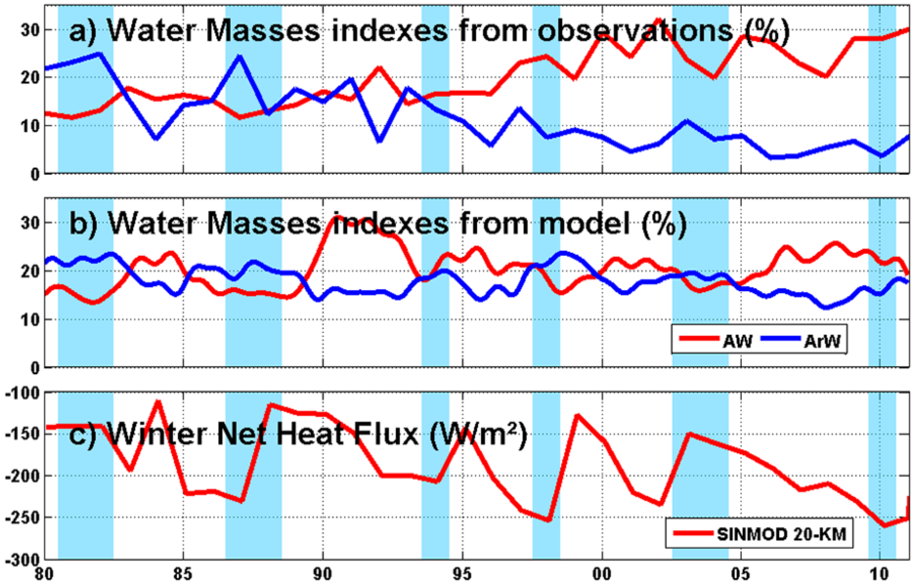

Figure 9. Inter-annual variations from 1980 to 2011 of **(a)** Atlantic Waters (AW) and Arctic Waters (ArW) index from in-situ observations and **(b)** from the SINMOD model (a low-passed filter (14 months) has been applied). **(c)** Winter (March) net heat fluxes from the SINMOD model.

OSD
12, 449–492, 2015

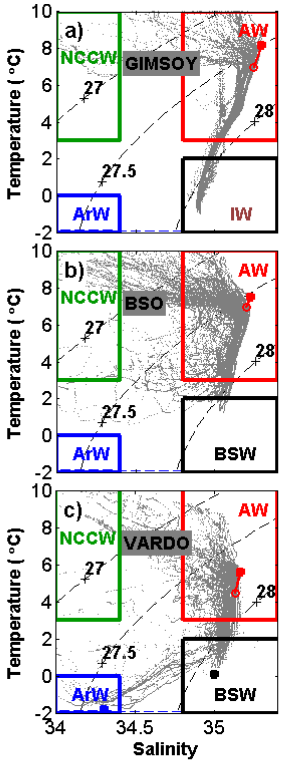

Figure 10. Potential temperature–salinity diagrams during the summer 2006–2011 period and shifts in the characteristics of the "ideal water masses" from the 1980–1985 period for: **(a)** Gimsoy section **(b)** BSO section and **(c)** Vardø section. Red: ideal Atlantic Water, black: ideal Barents Sea Water and blue: ideal Arctic Water. Intermediate Arctic Waters: IW.

OSD
12, 449–492, 2015

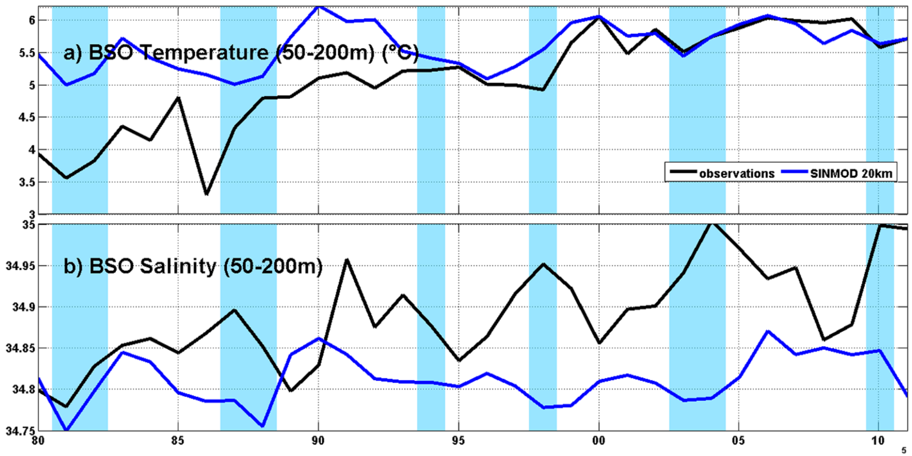

Figure 11. Time series from 1980 to 2011 of: **(a)** the temperature and **(b)** salinity (50–200 m) at BSO section from observations (black), SINMOD model (blue).

OSD
12, 449–492, 2015

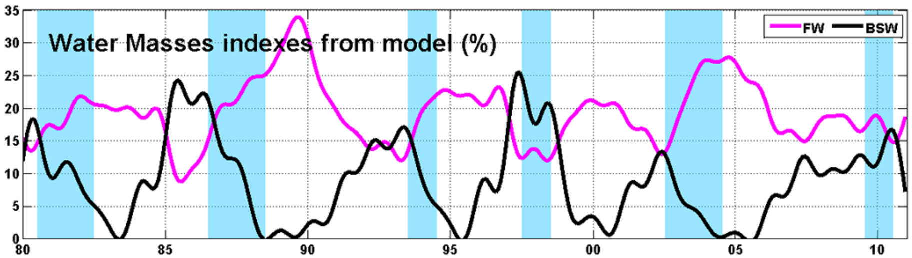

Figure 12. Inter-annual variations from 1980 to 2011 of Barents Sea Waters (BSW) and Fresh Waters (FW) index from the SINMOD model. A low-passed filter (14 months) has been applied.

OSD
12, 449–492, 2015

The Barents Sea polar front and water masses variability (1980–2011)

L. Oziel et al.

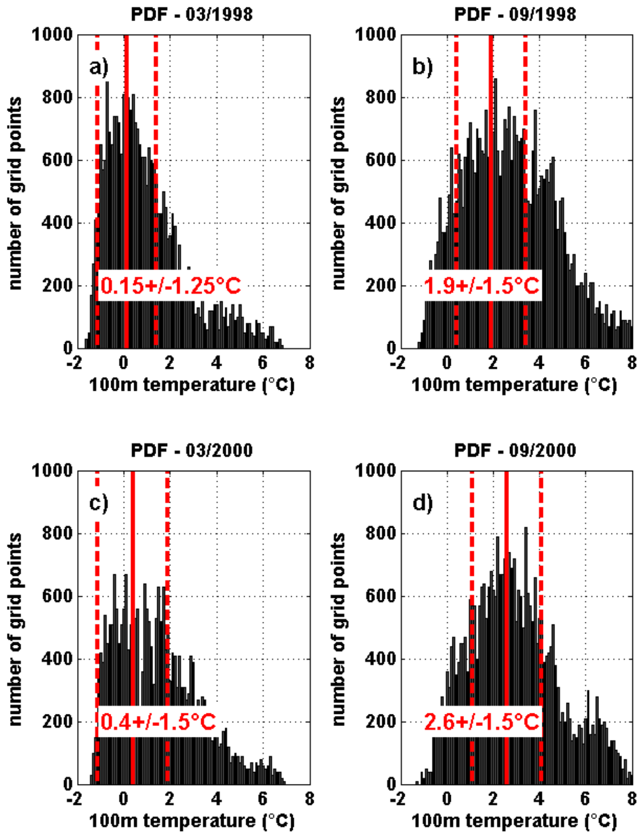

Figure 13. Probability Density Functions (PDF) of the temperature fields (the period is indicated above each panel).

OSD
12, 449–492, 2015

The Barents Sea polar front and water masses variability (1980–2011)

L. Oziel et al.

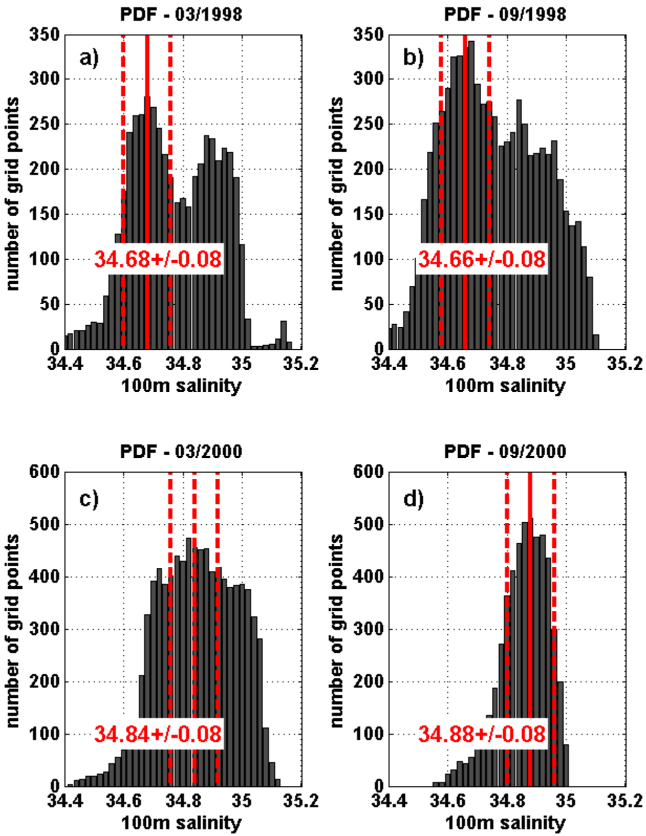

Figure 14. Probability Density Functions (PDF) of the salinity fields (the period is indicated above each panel).

OSD
12, 449–492, 2015

The Barents Sea polar front and water masses variability (1980–2011)

L. Oziel et al.

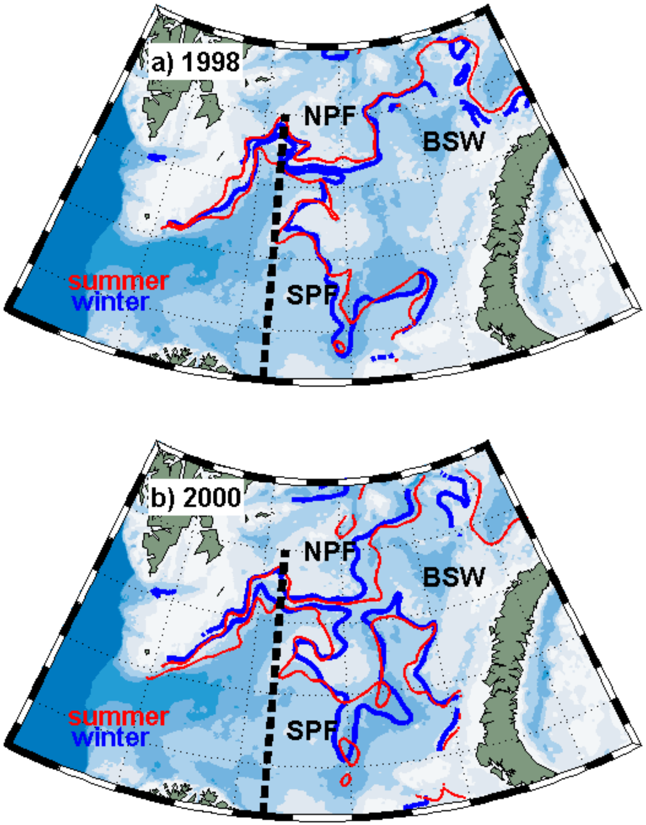

Figure 15. Seasonal and inter-annual variability of the "South Polar Front" (SPF) and "North Polar Front" (NPF). **(a)** 1998 and **(b)** 2000; (red line: summer; blue line: winter). The bathymetry and Vardø Section are shown.

OSD
12, 449–492, 2015

The Barents Sea polar front and water masses variability (1980–2011)

L. Oziel et al.